Electronic Research Archive

https://www.aimspress.com/journal/era

ERA, 34(4): 2607–2630.
DOI: 10.3934/era.2026121
Received: 26 January 2026
Revised: 14 March 2026
Accepted: 17 March 2026
Published: 25 March 2026

Research article

Hybrid impulsive synchronization control of heterogeneous neural networks under dynamic and static event-triggered conditions

Chengyi Jia[1], **Sijiao Sun**[1], **Fang Han**[1,2,*] **and Xiaoyan Liu**[1,*]

[1] School of Information and Intelligent Sciences, Donghua University, Shanghai 201620, China
[2] School of Mathematics and Statistics, Ningxia University, Yinchuan 750021, China

* **Correspondence:** Email: yadiahan@163.com, liuxy@dhu.edu.cn.

Abstract: To address the synchronization control problem of heterogeneous neural networks, this paper proposed a novel adaptive impulsive hybrid control strategy incorporating state feedback and event-triggered mechanisms. First, based on Lyapunov stability theory, the effectiveness of the designed controller was established under a static event-triggered scheme, achieving synchronization of heterogeneous neural networks while avoiding Zeno behavior. Then, an auxiliary parameter was introduced to dynamically adjust the triggering threshold, thereby constructing a dynamic event-triggered mechanism. On the basis of the static triggering principle, the validity of the controller under the dynamic event-triggered condition was further verified. Finally, numerical simulations were conducted to demonstrate the effectiveness and feasibility of the proposed method. The results show that, compared with the traditional static triggering strategy, the dynamic event-triggered scheme can guarantee synchronization performance while significantly reducing the number of triggering events and lowering system resource consumption, thereby validating the advantages of the proposed approach.

Keywords: heterogeneous neural networks; impulsive control; dynamic event-triggered mechanism; Zeno behavior; synchronization

1. Introduction

Neural networks, as a special class of complex networks, originate from the abstraction and modeling of biological neural systems. They exhibit fundamental properties such as nonlinearity, self-adaptation, robustness, and fault tolerance, which are intrinsic characteristics of real neural circuits [1, 2]. By bridging biological plausibility with mathematical modeling, neural networks have emerged as powerful tools for exploring neural information processing, brain-inspired computation, and learning mechanisms [3]. Due to their broad potential applications in signal processing, image

recognition, and large-scale language models, neural networks have attracted substantial attention across multiple scientific disciplines [4–6]. In the existing studies on neural networks, homogeneous neural networks are the most commonly analyzed because the dynamic behaviors of nodes with identical structures or nonlinearities are consistent, making analysis relatively simple. However, many real-world systems are inherently heterogeneous, and research on such systems has gradually increased [7–11]. For heterogeneous neural networks, each node may exhibit different dynamical behaviors, which leads to greater complexity and uncertainty. Therefore, studying heterogeneous neural networks is more meaningful [12]. A network is considered heterogeneous when the nodes exhibit nonidentical dynamics, which may arise from differences in system parameters, activation functions, or external inputs [13]. At present, research on heterogeneous neural networks remains limited, and synchronization control of heterogeneous networks is an important topic worthy of further investigation.

Although many control methods have been developed for synchronization in homogeneous neural networks [14], such as adaptive control [15, 16], sliding-mode control [17, 18], intermittent control [19, 20], and pinning control, most of them are designed for systems with identical node dynamics. However, for heterogeneous neural networks, where nodes may exhibit different dynamical properties, a single control strategy may not fully exploit the advantages of different methods. Therefore, integrating multiple control strategies to form hybrid control schemes has attracted increasing attention. For complex networks, traditional continuous control strategies require frequent acquisition and transmission of system states, resulting in high communication cost. Compared with traditional continuous control, impulsive control achieves synchronization of delayed neural networks with mismatched parameters at fixed discrete times. This method effectively reduces energy consumption by avoiding continuous communication and frequent triggering [21, 22]. Following this, Zhou et al. [23] further proposed an event-triggered impulsive control strategy to reduce transmission delays and improve synchronization accuracy. Later, Zhou et al. introduced a novel event-triggered impulsive control scheme based on communication delays and switching thresholds, which significantly reduced triggering frequency and improved control efficiency [24].

Therefore, combining impulsive control with event-triggered mechanisms can further reduce unnecessary control updates and communication transmissions, while maintaining effective synchronization performance, which provides a promising approach for synchronization control of heterogeneous neural networks. Since the concept of event-triggered control was introduced over the past two decades [23–25], it has been widely used to save communication and computational resources [10, 21, 26]. Under time-triggered strategies, system states must be transmitted periodically, whereas event-triggered mechanisms can effectively reduce system energy consumption by transmitting state information only when necessary. Various event-triggered mechanisms have been proposed, such as distributed event triggering [26], self-triggered control [27], adaptive event triggering [23], and event-triggered impulsive control [25]. Compared with static triggering strategies, dynamic triggering strategies introduce an auxiliary parameter to adjust the threshold function at each triggering moment, effectively reducing unnecessary triggering events and saving energy.

However, despite the progress achieved in synchronization control of neural networks, several issues still deserve further investigation. Most existing results mainly focus on homogeneous neural networks, where the dynamical properties of nodes are identical, which simplifies the synchronization analysis. In many practical applications, neural networks often exhibit heterogeneous dynamics due to differences

in system parameters, activation functions, or external inputs. Moreover, although event-triggered impulsive control has been introduced to reduce communication burden, most existing studies are still based on static event-triggered schemes. Research on heterogeneous neural networks under dynamic event-triggered impulsive control remains relatively limited, which motivates the work in this paper.

The considered drive-response neural network structure is inspired by the master–slave framework commonly encountered in practical networked control systems. Due to differences in hardware implementation, parameter configurations, or nonlinear characteristics, the dynamics of the drive and response systems are often not identical, which motivates modeling them as heterogeneous neural networks.

Based on the above discussion and the control structure illustrated in Figure 1, this paper investigates the synchronization control of heterogeneous neural networks and proposes a novel hybrid control strategy. The main contributions are as follows:

i. Unlike most existing studies that focus on homogeneous neural networks [10, 21, 24], the heterogeneous neural network considered in this paper features nodes with distinct dynamical properties. Compared with homogeneous networks, studying heterogeneous neural networks is more meaningful from both theoretical and practical perspectives.
ii. A novel adaptive hybrid control strategy combining state feedback and impulsive control with event-triggered mechanisms is proposed. Based on Lyapunov stability theory, impulsive comparison techniques and parameter variation methods are adopted to rigorously prove that the proposed controller ensures synchronization while effectively reducing the triggering frequency and shortening the control time, thereby improving control efficiency.
iii. Both static and dynamic event-triggered mechanisms are developed to achieve synchronization of heterogeneous neural networks. In particular, under the dynamic event-triggered scheme, synchronization can still be ensured even though existing studies on heterogeneous neural networks under dynamic event-triggered conditions remain limited. By introducing an auxiliary parameter to adjust the threshold function, a new dynamic event-triggered mechanism is established. This mechanism avoids frequent triggering present in traditional static strategies, reduces energy consumption, and fully demonstrates the effectiveness and engineering potential of the proposed control scheme.

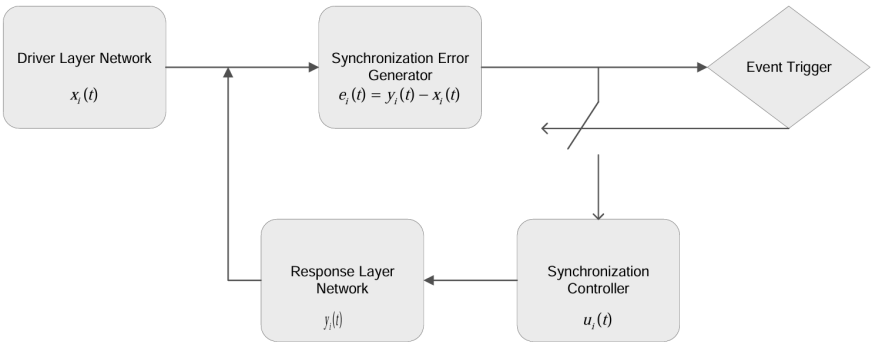

Figure 1. Control framework of the heterogeneous neural network under hybrid event-triggered impulsive control.

2. Lemmas and assumptions

Let $\mathbb{R}$ be the set of real numbers. $\mathbb{R}^n$ and $\mathbb{R}^{n\times m}$ denote the sets of n-dimensional real column vectors and $n \times m$ real matrices. E is the $N \times N$ identity matrix, A^T denotes the transpose of a matrix or vector A, and $diag\{d_1, d_2, \cdots, d_n\}$ denotes an n-dimensional diagonal matrix. $\lambda_{\min}(A)$ and $\lambda_{\max}(A)$ denote the minimum and maximum eigenvalues of the symmetric matrix A. $\|\cdot\|$ denotes the vector or matrix 2-norm. PC(n) is the set of piecewise continuous functions. For $\chi(t^+) = \lim_{s\to 0^+}\chi(t+s)$ and $\chi(t^-) = \lim_{s\to 0^-}\chi(t+s)$, $D^+\chi(t) = \limsup_{s\to 0^+}\frac{\chi(t+s)-\chi(t)}{s}$.

Lemma 1 [28]. If there exist $z_i(t), \tilde{z}_i(t) \in$ PC(1) such that $t = t_s^i$ is a discontinuity point, $z_i(t_s^{i-})$ and $\tilde{z}_i(t_s^{i-})$ exist, and $z_i(t_s^{i+}) = z_i(t_s^{i-})$, $\tilde{z}_i(t_s^{i+}) = \tilde{z}_i(t_s^{i-})$, then there exist positive constants $a_1, a_2 > 0$ and $\tilde{\rho} > 0$ such that

$$\begin{cases} D^+z_i(t) \le a_1 z_i(t) + a_2 z_i(t-\tau), & t \ne t_s^i,\ t > 0, \\ z_i(t_s^{i+}) \le \tilde{\rho} z_i(t_s^{i-}), & s \in \mathbb{N}, \end{cases}$$

and

$$\begin{cases} D^+\tilde{z}_i(t) \ge a_1 \tilde{z}_i(t) + a_2 \tilde{z}_i(t-\tau), & t \ne t_s^i,\ t > 0, \\ \tilde{z}_i(t_s^{i+}) = \tilde{\rho} \tilde{z}_i(t_s^{i-}), & s \in \mathbb{N}. \end{cases}$$

If $z_i(t) \le \tilde{z}_i(t)$ for all $t \in [-\tau, 0]$, then $z_i(t) \le \tilde{z}_i(t)$ holds for all $t > 0$.

Assumption 1. For the activation functions $f_i^M(\cdot)$, $f_i^S(\cdot)$, $g_i^M(\cdot)$, and $g_i^S(\cdot)$ of the network system, there exist positive constants $\alpha_{ik}^M, \alpha_{ik}^S, \beta_{ik}^M, \beta_{ik}^S$ such that

$$|f_i^M(p) - f_i^M(q)| \le \alpha_{ik}^M |p-q|, \qquad |f_i^S(p) - f_i^S(q)| \le \alpha_{ik}^S |p-q|,$$

$$|g_i^M(p) - g_i^M(q)| \le \beta_{ik}^M |p-q|, \qquad |g_i^S(p) - g_i^S(q)| \le \beta_{ik}^S |p-q|.$$

Here $i = 1, 2, \ldots, N$, $k = 1, 2, \ldots, n$. Define the diagonal matrices

$$\Xi_1^i = \text{diag}\{\alpha_{i1}^M, \ldots, \alpha_{in}^M\}, \quad \Xi_2^i = \text{diag}\{\alpha_{i1}^S, \ldots, \alpha_{in}^S\},$$

$$\Xi_3^i = \text{diag}\{\beta_{i1}^M, \ldots, \beta_{in}^M\}, \quad \Xi_4^i = \text{diag}\{\beta_{i1}^S, \ldots, \beta_{in}^S\}.$$

Definition 1 [29]. For a drive-response network with N nodes, let $x_i(t)$ and $y_i(t)$ represent the states of the drive layer and the corresponding response layer. If for any initial conditions, the network satisfies

$$\lim_{t\to\infty} \|x_i(t) - y_i(t)\| = 0 \qquad (i = 1, 2, \ldots, N),$$

then the network achieves complete synchronization. If instead $\limsup_{t\to\infty} \|x_i(t) - y_i(t)\| \le c (i = 1, 2, \ldots, N)$, for some constant $c > 0$, then the network achieves quasi-synchronization.

Remark 1. For heterogeneous neural networks, the node dynamics may differ due to parameter mismatches, structural differences, and heterogeneous activation functions. Under such conditions, achieving complete synchronization is often difficult in practical systems. Therefore, quasi-synchronization provides a more realistic performance objective, where the synchronization errors converge to a bounded neighborhood of zero. From an engineering perspective, this means that the states of the drive and response layers remain consistent within an acceptable tolerance range, which is sufficient for many applications requiring coordinated behavior.

Definition 2 [30]. If there exists a constant $\rho_1 > 0$ such that the impulse interval satisfies $\inf_{s\in\mathbb{N}}\{t_s - t_{s-1}\} \ge \rho_1 > 0$, then the synchronization error system does not exhibit Zeno behavior.

3. Synchronization analysis under a static event-triggered mechanism

3.1. Synchronization error system of heterogeneous neural networks

Consider a heterogeneous neural network in which the drive layer and the response layer each contain N nodes. The considered structure follows a drive-response synchronization framework, where each node in the response layer is required to track the corresponding node in the drive layer. The network dynamics are described as follows:

$$\begin{cases} \dot{x}_i(t) = -C_i^M x_i(t) + A_i^M f^M(x_i(t)) + B_i^M g^M(x_i(t-\tau)) + J, \\ \dot{y}_i(t) = -C_i^S y_i(t) + A_i^S f^S(y_i(t)) + B_i^S g^S(y_i(t-\tau)) + J + u_i(t), \end{cases} \tag{3.1}$$

where $i = 1, 2, \ldots, N$, and $x_i(t), y_i(t) \in \mathbb{R}^n$ represent the states of the i-th neuron in the drive layer and response layer, respectively. Functions $f^M(\cdot)$, $f^S(\cdot)$, $g^M(\cdot)$, $g^S(\cdot) : \mathbb{R}^n \to \mathbb{R}^n$ are activation functions. Matrices A_i^M, A_i^S, B_i^M, B_i^S are constant matrices. $C_i^M = \text{diag}\{C_{i1}^M, C_{i2}^M, \ldots, C_{in}^M\}$ and $C_i^S = \text{diag}\{C_{i1}^S, C_{i2}^S, \ldots, C_{in}^S\}$ are diagonal connection weight matrices. $J \in \mathbb{R}^n$ denotes an external input vector, $\tau > 0$ is the time delay, and $u_i(t) \in \mathbb{R}^n$ is the control input for the i-th neuron.

Define the synchronization error between the drive and response layers as $e_i(t) = y_i(t) - x_i(t)$, $i = 1, 2, \ldots, N$. Differentiating yields

$$\begin{aligned} \dot{e}_i(t) &= \dot{y}_i(t) - \dot{x}_i(t) \\ &= -C_i^S y_i(t) + A_i^S f^S(y_i(t)) + B_i^S g^S(y_i(t-\tau)) \\ &\quad - \Big[- C_i^M x_i(t) + A_i^M f^M(x_i(t)) + B_i^M g^M(x_i(t-\tau)) \Big] + u_i(t) \\ &= -C_i^S e_i(t) + A_i^S (f^S(y_i(t)) - f^S(x_i(t))) \\ &\quad + B_i^S (g^S(y_i(t-\tau)) - g^S(x_i(t-\tau))) + F_i(x_i(t)) + u_i(t), \end{aligned} \tag{3.2}$$

where the mismatch function between the drive and response layers is defined as $F_i(x_i(t)) = (C_i^M - C_i^S)x_i(t) + (A_i^S f^S(x_i(t)) - A_i^M f^M(x_i(t))) + (B_i^S g^S(x_i(t-\tau)) - B_i^M g^M(x_i(t-\tau)))$.

3.2. Static event-triggered control protocol

The event-triggered mechanism can effectively save communication resources and avoid continuous transmission of information. Therefore, a control protocol based on a static event-triggered mechanism is designed.

$$u_i(t) = -k e_i(t_s^i) + \sum_{s=1}^{+\infty} \left(\rho_s^{(i)} - 1\right) e_i(t_s^i)\, \delta(t - t_s^i), \quad t \in [t_{s-1}^i, t_s^i), \ s \in \mathbb{N}, \tag{3.3}$$

where $i = 1, 2, \ldots, N$, t_s^i is the event-triggering instant, $t_0 = 0$ is the initial time, $\{t_1, t_2, t_3, \ldots\}$ is the sequence of triggering times, k is the feedback control gain, $\rho_s^{(i)}$ is the impulsive strength, and $\delta(\cdot)$ is the Dirac delta function.

Remark 2. The second design item in (3.3) corresponds to the impulsive control component introduced at the event-triggering instants. Its main function is to instantaneously correct the synchronization error so as to compensate for the performance degradation caused by the event-triggered sampling mechanism. In coordination with the continuous state-feedback term, this impulsive correction helps

accelerate the error convergence. Moreover, it contributes to reducing the event-triggering frequency, thereby improving the overall control efficiency and facilitating the subsequent stability analysis.

Assume that at $t = t_s^i$, $e_i(t_s^{i+}) = e_i(t_s^{i-})$. The error system of the state feedback and impulsive control based on the static event-triggered mechanism is given by:

$$\begin{cases} \dot{e}_i(t) = -C_i^S e_i(t) + A_i^S \left(f^S(y_i(t)) - f^S(x_i(t))\right) + B_i^S \left(g^S(y_i(t-\tau)) - g^S(x_i(t-\tau))\right) \\ \qquad\quad + F_i(x_i(t)) - k\, e_i\left(t_s^i\right), \qquad t \in \left[t_{s-1}^i,\, t_s^i\right),\ s \in \mathbb{N}, \\ e_i\left(t_s^{i+}\right) = \rho_s^{(i)}\, e_i\left(t_s^{i-}\right), \qquad s \in \mathbb{N}. \end{cases} \tag{3.4}$$

Remark 3. The impulsive sequence is non-periodic and determined by the event-triggering condition. Thus, event-triggered impulsive control not only reduces communication burden but also makes full use of available network resources.

3.3. Synchronization analysis procedure of neural networks under static event-triggered conditions

Theorem 1. If Assumption 1 holds and the following static event-triggering conditions are satisfied, then the heterogeneous neural network achieves quasi-synchronization:

$$\lambda_{\max}(\Lambda_1^i) > 0, \qquad \lambda_{\max}(\Lambda_2^i) > 0.$$

The event-triggering instants are denoted by t_s^i, and the event-triggering function is defined as

$$t_{s+1}^i = \inf\left\{t > t_s^i \;\middle|\; \|e_i(t)\|^2 - \|e_i(t_s^i)\|^2 < 0\right\}. \tag{3.5}$$

Remark 4. The event-triggered control protocol proposed in this subsection is static. Intuitively, the static event-triggering condition compares the current synchronization error with the error at the last triggering instant, and a triggering event occurs only when the deviation becomes sufficiently large, thereby avoiding unnecessary control updates. A new dynamic event-triggered protocol will be presented later. Compared with the static mechanism, the dynamic event-triggered strategy introduces an auxiliary variable to adaptively adjust the triggering threshold, which can further reduce the triggering frequency while preserving synchronization performance. Since dynamic event-triggered control includes impulsive effects, the synchronization proof for dynamic triggering relies on the results of static event triggering.

Proof. Construct the Lyapunov function

$$V_1(t) = \sum_{i=1}^{N} V_i(t) = \sum_{i=1}^{N} [e_i^T(t) e_i(t)], \qquad i = 1, 2, \ldots, N. \tag{3.6}$$

Taking the upper-right Dini derivative of $V_i(t)$ yields

$$
\begin{aligned}
D^+V_1(t) = & \sum_{i=1}^{N}\Big[2e_i^{\mathrm{T}}(t)\Big(- C_i^S e_i(t) + A_i^S(f^S(y_i(t)) - f^S(x_i(t))) \\
& + B_i^S(g^S(y_i(t-\tau)) - g^S(x_i(t-\tau))) + F_i(x_i(t))\Big) - 2ke_i^{\mathrm{T}}(t)e_i(t_s^i)\Big] \\
\le & \sum_{i=1}^{N}\Big[e_i^{\mathrm{T}}(t)(- 2C_i^S)e_i(t) + e_i^{\mathrm{T}}(t)A_i^S(A_i^S)^{\mathrm{T}}e_i(t) \\
& + (f^S(y_i(t)) - f^S(x_i(t)))^{\mathrm{T}}(f^S(y_i(t)) - f^S(x_i(t))) + e_i^{\mathrm{T}}(t)B_i^S(B_i^S)^{\mathrm{T}}e_i(t) \\
& + (g^S(y_i(t-\tau)) - g^S(x_i(t-\tau)))^{\mathrm{T}}(g^S(y_i(t-\tau)) - g^S(x_i(t-\tau))) \\
& + e_i^{\mathrm{T}}(t)e_i(t) + F_i^{\mathrm{T}}(x_i(t))F_i(x_i(t)) - 2ke_i^{\mathrm{T}}(t)e_i(t_s^i)\Big] \\
\le & \sum_{i=1}^{N}\Big[e_i^{\mathrm{T}}(t)(- 2C_i^S + A_i^S(A_i^S)^{\mathrm{T}} + B_i^S(B_i^S)^{\mathrm{T}} + \left(\Xi_2^i\right)^2 + E)e_i(t) \\
& + e_i^{\mathrm{T}}(t-\tau)\left(\Xi_4^i\right)^2 e_i(t-\tau) + F_i^{\mathrm{T}}(x_i(t))F_i(x_i(t)) - 2ke_i^{\mathrm{T}}(t)e_i(t_s^i)\Big].
\end{aligned}
\tag{3.7}
$$

Using inequality techniques, one obtains

$$
\begin{aligned}
-2k\, e_i^{\mathrm{T}}(t)\, e_i(t_s^i) &= 2k\Big[(e_i(t_s^i) - e_i(t))^{\mathrm{T}}e_i(t_s^i) - e_i^{\mathrm{T}}(t_s^i)e_i(t_s^i)\Big] \\
&\le k\Big[(e_i(t_s^i) - e_i(t))^{\mathrm{T}}(e_i(t_s^i) - e_i(t)) - e_i^{\mathrm{T}}(t_s^i)e_i(t_s^i)\Big],
\end{aligned}
$$

and thus

$$
\begin{aligned}
D^+V_1(t) \le & \sum_{i=1}^{N}\Big[e_i^{\mathrm{T}}(t)(-2C_i^S + A_i^S(A_i^S)^{\mathrm{T}} + B_i^S(B_i^S)^{\mathrm{T}} + \left(\Xi_2^i\right)^2 + E)e_i(t) \\
& + e_i^{\mathrm{T}}(t-\tau)\left(\Xi_4^i\right)^2 e_i(t-\tau) + F_i^{\mathrm{T}}(x_i(t))\, F_i(x_i(t)) \\
& + k(e_i(t_s^i) - e_i(t))^{\mathrm{T}}(e_i(t_s^i) - e_i(t)) - ke_i^{\mathrm{T}}(t_s^i)\, e_i(t_s^i)\Big] \\
\le & \sum_{i=1}^{N}\Big[\lambda_{\max}(\Lambda_1^i)\, e_i^{\mathrm{T}}(t)e_i(t) + \lambda_{\max}(\Lambda_2^i)\, e_i^{\mathrm{T}}(t-\tau)e_i(t-\tau) \\
& + k(e_i(t_s^i) - e_i(t))^{\mathrm{T}}(e_i(t_s^i) - e_i(t)) - ke_i^{\mathrm{T}}(t_s^i)\, e_i(t_s^i) + F_i^{\mathrm{T}}(x_i(t))F_i(x_i(t))\Big] \\
\le & \sum_{i=1}^{N}\Big[\lambda_{\max}(\Lambda_1^i)\|e_i(t)\|^2 + \lambda_{\max}(\Lambda_2^i)\|e_i(t-\tau)\|^2 + \|F_i(x_i(t))\|^2\Big].
\end{aligned}
\tag{3.8}
$$

From the event-triggering condition, we have

$$
\|e_i(t_s^i) - e_i(t)\|^2 - \|e_i(t_s^i)\|^2 < 0.
$$

Thus,

$$\begin{aligned} D^+V_1(t) &\le \sum_{i=1}^{N}\Big[\lambda_{\max}(\Lambda_1^i)\|e_i(t)\|^2 + \lambda_{\max}(\Lambda_2^i)\|e_i(t-\tau)\|^2 + \|F_i(x_i(t))\|^2\Big] \\ &\le \sum_{i=1}^{N}\Big[\lambda_{\max}(\Lambda_1^i)V_i(t) + \lambda_{\max}(\Lambda_2^i)V_i(t-\tau) + \gamma\Big]. \end{aligned} \tag{3.9}$$

Let $\Lambda_1^i = -2C_i^S + A_i^S(A_i^S)^{\mathrm{T}} + B_i^S(B_i^S)^{\mathrm{T}} + \Xi_2^{i2} + E,\ \Lambda_2^i = \Xi_4^{i2},\ i \in \{1, 2, \ldots, N\},\ \gamma = \|F_i(x_i(t))\|^2$. Construct the auxiliary function

$$\begin{cases} D^+z_i(t) = c_1z_i(t) + c_2z_i(t-\tau) + \gamma + \omega, & t \ne t_s^i,\ t > 0, \\ z_i(t_s^{i+}) = \rho_s^{(i)}z_i(t_s^{i-}), & t = t_s^i,\ s \in \mathbb{N}, \\ z_i(t) = V_i(t), & -\tau \le t \le 0. \end{cases} \tag{3.10}$$

According to the lemma, $V_i(t) \le z_i(t)$ for $t \ge 0$. From the parametric representation of $z_i(t)$, one obtains

$$z_i(t) = W_i(t,0)\,z_i(0) + \int_0^t W_i(t,r)(c_2z_i(r-\tau) + \gamma + \omega)dr, \quad t > 0. \tag{3.11}$$

Here $W(t,r)$ denotes the Cauchy matrix of the following impulsive differential equation:

$$\begin{cases} D^+z_i(t) = c_1z_i(t), & t \ne t_s^i,\ t > 0, \\ z_i(t_s^{i+}) = \rho_s^{(i)}z_i(t_s^{i-}), & t = t_s^i, s \in \mathbb{N}. \end{cases} \tag{3.12}$$

By mathematical induction, we have

$$W_i(t,r) = e^{c_1(t-r)}\left(\prod_{r<t_s^i<t}\rho_s^{(i)}\right). \tag{3.13}$$

Since $0 < \rho_s^{(i)} < 1$, let $\rho = \max\{\rho_s^{(i)}\} < 1$. There exists a constant ν such that $\inf_{s\in\mathbb{N}}(t_s - t_{s-1}) \ge \nu > 0$. Therefore,

$$W_i(t,r) \le (\rho_s^{(i)})^{\frac{t-r}{\nu}}e^{c_1(t-r)} \le \frac{1}{\rho}e^{(c_1+\ln\rho)(t-r)}. \tag{3.14}$$

From the above results, one obtains

$$\begin{aligned} z_i(t) &\le \frac{1}{\rho}e^{\left(c_1+\frac{\ln\rho}{\nu}\right)t}\|e_i(0)\| + \int_0^t \frac{1}{\rho}e^{\left(c_1+\frac{\ln\rho}{\nu}\right)(t-r)}(c_2z_i(r-\tau) + \gamma + \omega)\,dr \\ &\le \tilde{\mu}\,e^{\left(c_1+\frac{\ln\rho}{\nu}\right)t} + \int_0^t e^{\left(c_1+\frac{\ln\rho}{\nu}\right)(t-r)}\left(\frac{c_2}{\rho}z_i(r-\tau) + \frac{\gamma+\omega}{\rho}\right)dr, \end{aligned} \tag{3.15}$$

where $\tilde{\mu} = \rho^{-1}\sup_{-\tau\le v\le 0}\|e_i(v)\|$.

Define the auxiliary function $f(b) = b + \left(c_1 + \frac{\ln\rho}{\nu}\right) + \rho^{-1}c_2e^{b\tau}$. Since $f(0) < 0, f(+\infty) > 0$, and $-\left(c_1 + \frac{\ln\rho}{\nu}\right) > \rho^{-1}c_2 > 0$, as well as, $f'(b) = 1 + \tau\rho^{-1}c_2e^{b\tau} > 0$, it follows that there exists a unique solution for $b > 0$ such that $f(b) = 0$.

When $-\tau \le t \le 0$, since $b > 0$, $\omega > 0$, and $0 < \rho < 1$, one has

$$z_i(t) \le \tilde{\mu} e^{\left(c_1 + \frac{\ln \rho}{\nu}\right)t} < \tilde{\mu} e^{-bt} + \frac{\rho^{-1}(\gamma + \omega)}{-\left(c_1 + \frac{\ln \rho}{\nu}\right) - \rho^{-1} c_2}. \tag{3.16}$$

When $t > 0$, it is required to prove that the following inequality holds:

$$z_i(t) < \tilde{\mu} e^{-bt} + \frac{\rho^{-1}(\gamma + \omega)}{-\left(c_1 + \frac{\ln \rho}{\nu}\right) - \rho^{-1} c_2}. \tag{3.17}$$

If the above inequality does not hold, then there exists $t^* > 0$ such that

$$z_i(t^*) \ge \tilde{\mu} e^{-bt^*} + \frac{\rho^{-1}(\gamma + \omega)}{-\left(c_1 + \frac{\ln \rho}{\nu}\right) - \rho^{-1} c_2}. \tag{3.18}$$

Moreover, for $t < t^*$, one has

$$z_i(t) < \tilde{\mu} e^{-bt} + \frac{\rho^{-1}(\gamma + \omega)}{-\left(c_1 + \frac{\ln \rho}{\nu}\right) - \rho^{-1} c_2}. \tag{3.19}$$

Combining the above results, one obtains

$$\begin{aligned}
z_i(t^*) &\le \tilde{\mu} e^{\left(c_1 + \frac{\ln \rho}{\nu}\right)t^*} + \int_0^{t^*} e^{\left(c_1 + \frac{\ln \rho}{\nu}\right)(t^* - r)} \left(\rho^{-1} c_2 z_i(r - \tau) + \rho^{-1}(\gamma + \omega)\right) dr \\
&< e^{\left(c_1 + \frac{\ln \rho}{\nu}\right)t^*} \left\{ \tilde{\mu} + \frac{\rho^{-1}(\gamma + \omega)}{-\left(c_1 + \frac{\ln \rho}{\nu}\right) - \rho^{-1} c_2} + \int_0^{t^*} e^{-\left(c_1 + \frac{\ln \rho}{\nu}\right)r} \left(\rho^{-1} c_2 z_i(r - \tau) + \rho^{-1}(\gamma + \omega)\right) dr \right\} \\
&< e^{\left(c_1 + \frac{\ln \rho}{\nu}\right)t^*} \left\{ \tilde{\mu} + \frac{\rho^{-1}(\gamma + \omega)}{-\left(c_1 + \frac{\ln \rho}{\nu}\right) - \rho^{-1} c_2} + \int_0^{t^*} e^{-\left(c_1 + \frac{\ln \rho}{\nu}\right)r} \Big[\rho^{-1} c_2 \Big(\tilde{\mu} e^{-b(r - \tau)} \right. \right. \\
&\qquad \left. \left. + \frac{\rho^{-1}(\gamma + \omega)}{-\left(c_1 + \frac{\ln \rho}{\nu}\right) - \rho^{-1} c_2} \Big) + \rho^{-1}(\gamma + \omega) \Big] dr \right\} \\
&< e^{\left(c_1 + \frac{\ln \rho}{\nu}\right)t^*} \left\{ \tilde{\mu} + \frac{\rho^{-1}(\gamma + \omega)}{-\left(c_1 + \frac{\ln \rho}{\nu}\right) - \rho^{-1} c_2} + \frac{\rho^{-1} c_2 \tilde{\mu}}{\left(c_1 + \frac{\ln \rho}{\nu}\right) - b} \Big[e^{b\tau} \left(e^{\left(c_1 + \frac{\ln \rho}{\nu}\right)t^*} - 1 \right) \Big] \right. \\
&\qquad \left. + \frac{\rho^{-1}(\gamma + \omega)}{-\left(c_1 + \frac{\ln \rho}{\nu}\right) - \rho^{-1} c_2} \Big[e^{-\left(c_1 + \frac{\ln \rho}{\nu}\right)t^*} - 1 \Big] \right\} \\
&\le \tilde{\mu} e^{-bt^*} + \frac{\rho^{-1}(\gamma + \omega)}{-\left(c_1 + \frac{\ln \rho}{\nu}\right) - \rho^{-1} c_2}.
\end{aligned} \tag{3.20}$$

When $\omega \to 0$, it follows that $V_i(t) \le z_i(t) \le \tilde{\mu} e^{-bt} + \frac{\rho^{-1}\gamma}{-\left(c_1 + \frac{\ln \rho}{\nu}\right) - \rho^{-1} c_2}, t \ge 0$. Therefore, the drive layer and the response layer can achieve quasi-synchronization.

3.4. Analysis of Zeno behavior under static event-triggering

Event-triggered control strategies may suffer from Zeno behavior, that is, infinitely many triggering events may occur within a finite time interval. Therefore, it is necessary to exclude the occurrence of Zeno behavior.

Define the measurement error variable as $\varepsilon_i(t) = e_i(t_s^i) - e_i(t)$, $i \in \{1, 2, \ldots, N\}$. Taking the derivative of $\varepsilon_i(t)$ yields

$$\begin{aligned}\dot{\varepsilon}_i(t) &= -\dot{e}_i(t)\\ &= -C_i^S e_i(t) - A_i^S\left(f^S(y_i(t)) - f^S(x_i(t))\right) - B_i^S\left(g^S(y_i(t-\tau)) - g^S(x_i(t-\tau))\right)\\ &\quad - F_i(x_i(t)) + ke_i(t_s^i), \qquad t \in [t_{s-1}^i, t_s^i),\ s \in \mathbb{N}.\end{aligned} \tag{3.21}$$

Theorem 2. Under the control protocol and the conditions of Theorem 1, the event-triggering interval satisfies $t_{s+1}^i - t_s^i > 0$, and thus the static event-triggered control scheme does not exhibit Zeno behavior.

Proof. Construct the Lyapunov function $V_2(t) = \varepsilon_i^T(t)\varepsilon_i(t), i \in \{1, 2, \ldots, N\}$. Taking the derivative of the Lyapunov function yields

$$\begin{aligned}\dot{V}_2(t) &= 2\varepsilon_i^T(t)\dot{\varepsilon}_i(t)\\ &= 2\varepsilon_i^T(t)\Big[-C_i^S\varepsilon_i(t) - A_i^S\left(f^S(y_i(t)) - f^S(x_i(t))\right)\\ &\qquad - B_i^S\left(g^S(y_i(t-\tau)) - g^S(x_i(t-\tau))\right) - F_i(x_i(t)) + ke_i(t_s^i)\Big]\\ &\le \varepsilon_i^T(t)\Big((C_i^S)^TC_i^S + A_i^S(A_i^S)^T + B_i^S(B_i^S)^T + E\Big)\varepsilon_i(t)\\ &\quad + e_i^T(t)((\Xi_2^i)^2 + E)e_i(t) + e_i^T(t-\tau)(\Xi_4^i)^2e_i(t-\tau)\\ &\quad + 2k\varepsilon_i^T(t)e_i(t_s^i) + F_i^T(x_i(t))F_i(x_i(t)).\end{aligned} \tag{3.22}$$

According to inequality theory, it follows that

$$2k\varepsilon_i^T(t)e_i(t_s^i) \le k(\|\varepsilon_i(t)\|^2 + \|e_i(t_s^i)\|^2).$$

From the above inequality, it follows that

$$\begin{aligned}\dot{V}_2(t) &\le \varepsilon_i^T(t)\Big[(C_i^S)^TC_i^S + A_i^S(A_i^S)^T + B_i^S(B_i^S)^T + E\Big]\varepsilon_i(t) + k\|\varepsilon_i(t)\|^2\\ &\quad + e_i^T(t)((\Xi_2^i)^2 + E)e_i(t) + e_i^T(t-\tau)(\Xi_4^i)^2e_i(t-\tau) + k\|e_i(t_s^i)\|^2 + \|F_i(x_i(t))\|^2\\ &\le \lambda_{\max}\Big((C_i^S)^TC_i^S + A_i^S(A_i^S)^T + B_i^S(B_i^S)^T + E\Big)\|\varepsilon_i(t)\|^2\\ &\quad + \lambda_{\max}((\Xi_2^i)^2 + E)\|e_i(t)\|^2 + \lambda_{\max}((\Xi_4^i)^2)\|e_i(t-\tau)\|^2\\ &\quad + k\|e_i(t_s^i)\|^2 + \|F_i(x_i(t))\|^2\\ &\le W_1V_2(t) + W_2 + k\|e_i(t_s^i)\|^2.\end{aligned} \tag{3.23}$$

Let $W_1 = \lambda_{\max}\Big(C_i^S(C_i^S)^T + A_i^S(A_i^S)^T + B_i^S(B_i^S)^T + E\Big) + k$, $W_2 = \lambda_{\max}((\Xi_2^i)^2 + E) + \lambda_{\max}((\Xi_4^i)^2)$. Applying the integrating factor method on the interval $[t_s^i, t]$, we obtain

$$V_2(t) \le \frac{W_2 + k\|e_i(t_s^i)\|^2}{W_1}(e^{W_1(t-t_s^i)} - 1). \tag{3.24}$$

According to the event-triggering condition, one has

$$\|e_i(t_s^i) - e_i(t)\|^2 = \|e_i(t)\|^2 - \|e_i(t_s^i)\|^2 \geq 0.$$

Therefore, one has

$$\|e_i(t)\|^2 \leq \frac{W_2 + k\|e_i(t_s^i)\|^2}{W_1}\left(e^{W_1(t-t_s^i)} - 1\right). \tag{3.25}$$

It follows that $t_{s+1}^i - t_s^i \geq \frac{1}{W_1}\ln\left(\frac{W_1\|e_i(t_s^i)\|^2}{W_2+k\|e_i(t_s^i)\|^2} + 1\right) > 0$. Hence, the controlled error system does not exhibit Zeno behavior.

4. Synchronization analysis under dynamic event-triggering

4.1. Control protocol and the dynamic event-triggering function

Compared with the traditional static event-triggered control, dynamic event-triggered control introduces an additional dynamic triggering variable, which allows the triggering condition to be adjusted adaptively. This mechanism improves the control efficiency while ensuring system stability. In the control protocol, the feedback gain is designed as an adaptive variable, enabling a more flexible response to system error variations.

The control protocol is given as follows:

$$u_i(t) = -k_i(t)e_i(t_s^i) + \sum_{k=1}^{\infty}\left(\rho_k^{(i)} - 1\right)e_i(t)\delta(t - t_k^{(i)}), \quad t \in \left[t_{k-1}^{(i)}, t_k^{(i)}\right), \ k \in \mathbb{N}. \tag{4.1}$$

Here, the adaptive gain $k_i(t)$ is bounded above by $\bar{k}_i$. The upper bound of the adaptive control gain parameter is defined as the feedback gain under the static event-triggered mechanism, that is, $\bar{k}_i = k$.

The adaptive gain updating law is given by

$$k_i(t) = \begin{cases} e_i^T(t_s^i)e_i(t_s^i), & k_i(t) \leq \bar{k}_i, \\ 0, & k_i(t) > \bar{k}_i. \end{cases} \tag{4.2}$$

The dynamic event-triggering function is defined as

$$\dot{\eta}_i(t) = -\xi_i\eta_i(t) + \sigma_i\left(\|e_i(t_s^i)\|^2 - \|e_i(t_s^i) - e_i(t)\|^2\right), \quad t \in [t_s^i, t_{s+1}^i), \tag{4.3}$$

where $\eta_i(t)$ satisfies $\eta_i(0) > 0$, $i = 1, 2, \ldots, N$, $\xi_i > 0$, $\sigma_i < 0$, and $\sigma_i - k_i < 0$.

Proposition 1. The dynamic variable of the event-triggering function satisfies $\eta_i(t) > 0$, $i = 1, 2, \ldots, N$.

Proof. Combining the above equations, one obtains

$$\dot{\eta}_i(t) > \frac{k_i\xi_i}{\sigma_i - k_i}\eta_i(t). \tag{4.4}$$

Let $\Phi = \frac{k_i\xi_i}{\sigma_i - k_i}$, and then

$$\dot{\eta}_i(t) > \Phi\eta_i(t). \tag{4.5}$$

It follows that

$$\eta_i(t) > e^{\Phi t}\eta_i(0) > 0. \tag{4.6}$$

4.2. Synchronization analysis of neural networks under dynamic event-triggering

Theorem 3. Suppose that Assumption 1 and the static event-triggering condition are satisfied. Then, the heterogeneous neural networks can achieve quasi-synchronization.

The dynamic event-triggering condition is defined as

$$t_{s+1}^i = \inf\left\{t > t_s^i \;\middle|\; \eta_i(t) \le \frac{1}{\xi_i}\left[(\sigma_i - \bar{k}_i)\|e_i(t_s^i)\|^2 + (\bar{k}_i - \sigma_i)\|e_i(t_s^i) - e_i(t)\|^2\right]\right\}. \tag{4.7}$$

Proof. Construct the following Lyapunov function:

$$V_3(t) = \sum_{i=1}^{N} \tilde{V}_i(t) = \sum_{i=1}^{N}\left[e_i^T(t)e_i(t) + \eta_i(t) + \frac{(k_i(t) - \bar{k}_i)^2}{2}\right], \quad i \in \{1, 2, \ldots, N\}, \tag{4.8}$$

where $\tilde{V}_i(t) = V_i(t) + \eta_i(t) + \frac{(k_i(t)-\bar{k}_i)^2}{2}$.

Taking the upper-right Dini derivative of $V_3(t)$ yields

$$\begin{aligned} D^+V_3(t) &= \sum_{i=1}^{N}\left[2e_i^T(t)\dot{e}_i(t) + \dot{\eta}_i(t) + (k_i(t) - \bar{k}_i)\dot{k}_i(t)\right] \\ &= \sum_{i=1}^{N}\Big[2e_i^T(t)\big(-C_i^S e_i(t) + A_i^S(f^S(y_i(t)) - f^S(x_i(t))) \\ &\qquad + B_i^S(g^S(y_i(t-\tau)) - g^S(x_i(t-\tau))) + F_i(x_i(t)) + u_i(t)\big) \\ &\qquad + \dot{\eta}_i(t) + (k_i(t) - \bar{k}_i)\dot{k}_i(t)\Big]. \end{aligned} \tag{4.9}$$

Substituting the above results yields

$$\begin{aligned} D^+V_3(t) &= \sum_{i=1}^{N}\Big[2e_i^T(t)\big(-C_i^S e_i(t) + A_i^S(f^S(y_i(t)) - f^S(x_i(t))) \\ &\qquad + B_i^S(g^S(y_i(t-\tau)) - g^S(x_i(t-\tau)))\big) + F_i(x_i(t)) + \dot{\eta}_i(t) \\ &\qquad - 2k_i(t)e_i^T(t)e_i(t_s^i) + (k_i(t) - \bar{k}_i)e_i^T(t_s^i)e_i(t_s^i)\Big] \\ &\le \sum_{i=1}^{N}\Big[e_i^T(t)\big(-2C_i^S\big)e_i(t) + e_i^T(t)A_i^S(A_i^S)^T e_i(t) \\ &\qquad + \big(f^S(y_i(t)) - f^S(x_i(t))\big)^T\big(f^S(y_i(t)) - f^S(x_i(t))\big) + e_i^T(t)B_i^S(B_i^S)^T e_i(t) \\ &\qquad + \big(g^S(y_i(t-\tau)) - g^S(x_i(t-\tau))\big)^T\big(g^S(y_i(t-\tau)) - g^S(x_i(t-\tau))\big) \\ &\qquad + e_i^T(t)e_i(t) + F_i^T(x_i(t))F_i(x_i(t)) + \dot{\eta}_i(t) - 2k_i(t)e_i^T(t)e_i(t_s^i) \\ &\qquad + (k_i(t) - \bar{k}_i)e_i^T(t_s^i)e_i(t_s^i)\Big] \\ &\le \sum_{i=1}^{N}\Big[e_i^T(t)\Big(-2C_i^S + A_i^S(A_i^S)^T + B_i^S(B_i^S)^T + (\Xi_2^i)^2 + E\Big)e_i(t) \\ &\qquad + e_i^T(t-\tau)(\Xi_4^i)^2 e_i(t-\tau) + F_i^T(x_i(t))F_i(x_i(t)) \\ &\qquad + \dot{\eta}_i(t) - 2k_i(t)e_i^T(t)e_i(t_s^i) + (k_i(t) - \bar{k}_i)e_i^T(t_s^i)e_i(t_s^i)\Big]. \end{aligned} \tag{4.10}$$

According to inequality theory, one has

$$\begin{aligned} -2k_i(t)e_i^T(t)e_i(t_s^i) &= 2k_i(t)\Big[(e_i(t_s^i)-e_i(t))^T e_i(t_s^i) - e_i^T(t_s^i)e_i(t_s^i)\Big] \\ &\le k_i(t)\Big[(e_i(t_s^i)-e_i(t))^T(e_i(t_s^i)-e_i(t)) - e_i^T(t_s^i)e_i(t_s^i)\Big]. \end{aligned} \tag{4.11}$$

Substituting the above inequality into $D^+V_3(t)$ yields

$$\begin{aligned} D^+V_3(t) \le & \sum_{i=1}^{N}\Big[\lambda_{\max}\Big(\Lambda_1^i\Big)e_i^T(t)e_i(t) + \lambda_{\max}\Big(\Lambda_2^i\Big)e_i^T(t-\tau)e_i(t-\tau) + \dot{\eta}_i(t) \\ & + k_i(t)(e_i(t_s^i)-e_i(t))^T(e_i(t_s^i)-e_i(t)) - \bar{k}_i e_i^T(t_s^i)e_i(t_s^i) + F_i^T(x_i(t))F_i(x_i(t))\Big] \\ \le & \sum_{i=1}^{N}\Big[\lambda_{\max}\Big(\Lambda_1^i\Big)\|e_i(t)\|^2 + \lambda_{\max}\Big(\Lambda_2^i\Big)\|e_i(t-\tau)\|^2 - \xi_i\eta_i(t) + (\sigma_i-\bar{k}_i)\|e_i(t_s^i)\|^2 \\ & + (\bar{k}_i-\sigma_i)\|e_i(t_s^i)-e_i(t)\|^2 + \|F_i(x_i(t))\|^2\Big]. \end{aligned} \tag{4.12}$$

From the event-triggering function, one has $-\xi_i\eta_i(t) + (\sigma_i-\bar{k}_i)\|e_i(t_s^i)\|^2 + (\bar{k}_i-\sigma_i)\|e_i(t_s^i)-e_i(t)\|^2 < 0$. Substituting the above inequality into the derivative of the Lyapunov function yields

$$\begin{aligned} D^+V_3(t) &\le \sum_{i=1}^{N}\Big[\lambda_{\max}(\Lambda_1^i)\|e_i(t)\|^2 + \lambda_{\max}(\Lambda_2^i)\|e_i(t-\tau)\|^2 + \|F_i(x_i(t))\|^2\Big] \\ &\le \sum_{i=1}^{N}\Big[\lambda_{\max}(\Lambda_1^i)V_i(t) + \lambda_{\max}(\Lambda_2^i)V_i(t-\tau) + \gamma\Big]. \end{aligned} \tag{4.13}$$

Remark 5. The synchronization proof under both dynamic and static event-triggered mechanisms is established by the Lyapunov function $\tilde{V}_i(t) = V_i(t) + \eta_i(t) + \frac{(k_i(t)-\bar{k}_i)^2}{2}$. Therefore, the Lyapunov-based synchronization analysis under the dynamic event-triggered mechanism follows the same structure as that under the static event-triggered mechanism. By invoking Lemma 1, it can be concluded that the heterogeneous neural network can achieve quasi-synchronization under the dynamic event-triggered condition, and the drive layer and the response layer converge to each other asymptotically.

4.3. Zeno behavior analysis under a dynamic event-triggered mechanism

Similar to the static event-triggered strategy, it is also necessary to prove that the system does not exhibit Zeno behavior under the dynamic event-triggered mechanism.

Define the measurement error as $\varepsilon_i(t) = e_i(t_s^i) - e_i(t)$, $i \in \{1, 2, \ldots, N\}$. Taking the derivative of $\varepsilon_i(t)$ yields

$$\begin{aligned} \dot{\varepsilon}_i(t) &= -\dot{e}_i(t) \\ &= -C_i^S e_i(t) - A_i^S(f^S(y_i(t)) - f^S(x_i(t))) - B_i^S(g^S(y_i(t-\tau)) - g^S(x_i(t-\tau))) \\ &\quad - F_i(x_i(t)) + k_i(t)e_i(t_s^i). \end{aligned} \tag{4.14}$$

Theorem 4. Under the control protocol and the conditions of Theorem 3, the event-triggering interval satisfies $t_{s+1}^i - t_s^i > 0$, and thus the dynamic event-triggered mechanism does not exhibit Zeno behavior.

Proof. Construct the Lyapunov function $V_4(t) = \varepsilon_i^T(t)\varepsilon_i(t), i \in \{1, 2, \ldots, N\}$. Taking the derivative of the Lyapunov function yields the following.

$$\begin{aligned}
\dot{V}_4(t) &= 2\varepsilon_i^T(t)\dot{\varepsilon}_i(t) \\
&= 2\varepsilon_i^T(t)\Big[- C_i^S e_i(t) - A_i^S(f^S(y_i(t)) - f^S(x_i(t))) \\
&\quad - B_i^S(g^S(y_i(t-\tau)) - g^S(x_i(t-\tau))) - F_i(x_i(t)) + k_i(t)e_i(t_s^i)\Big] \\
&\le \varepsilon_i^T(t)\Big[C_i^S(C_i^S)^T + A_i^S(A_i^S)^T + B_i^S(B_i^S)^T + E\Big]\varepsilon_i(t) \\
&\quad + e_i^T(t)\Big((\Xi_2^i)^2 + E\Big)e_i(t) + e_i^T(t-\tau)(\Xi_4^i)^2 e_i(t-\tau) \\
&\quad + 2k_i(t)\varepsilon_i^T(t)e_i(t_s^i) + F_i^T(x_i(t))F_i(x_i(t)).
\end{aligned} \tag{4.15}$$

By inequality theory, we have

$$2k_i(t)\,\varepsilon_i^T(t)\,e_i\left(t_s^i\right) \le k_i(t)\left(\|\varepsilon_i(t)\|^2 + \left\|e_i\left(t_s^i\right)\right\|^2\right) \le \bar{k}_i\left(\|\varepsilon_i(t)\|^2 + \left\|e_i\left(t_s^i\right)\right\|^2\right).$$

Substituting the above inequality, one can further obtain

$$\begin{aligned}
\dot{V}_4(t) &\le \varepsilon_i^T(t)\Big[C_i^S(C_i^S)^T + A_i^S(A_i^S)^T + B_i^S(B_i^S)^T + E\Big]\varepsilon_i(t) + \bar{k}_i\varepsilon_i^T(t)\varepsilon_i(t) \\
&\quad + e_i^T(t)\Big((\Xi_2^i)^2 + E\Big)e_i(t) + e_i^T(t-\tau)(\Xi_4^i)^2 e_i(t-\tau) \\
&\quad + \bar{k}_i e_i^T(t_s^i)e_i(t_s^i) + F_i^T(x_i(t))F_i(x_i(t)) \\
&\le \Big[\lambda_{\max}\Big(C_i^S(C_i^S)^T + A_i^S(A_i^S)^T + B_i^S(B_i^S)^T + E\Big) + \bar{k}_i\Big]\|\varepsilon_i(t)\|^2 \\
&\quad + \lambda_{\max}\Big((\Xi_2^i)^2 + E\Big)\|e_i(t)\|^2 + \lambda_{\max}\Big((\Xi_4^i)^2\Big)\|e_i(t-\tau)\|^2 \\
&\quad + \bar{k}_i\|e_i(t_s^i)\|^2 + \|F_i(x_i(t))\|^2 \\
&= W_1\|\varepsilon_i(t)\|^2 + W_2 + \bar{k}_i\|e_i(t_s^i)\|^2.
\end{aligned} \tag{4.16}$$

Integrating the above inequality yields

$$V_4(t) \le \frac{W_2 + \bar{k}_i\|e_i(t_s^i)\|^2}{W_1}(e^{W_1(t-t_s^i)} - 1). \tag{4.17}$$

According to the dynamic event-triggering condition, we have

$$\eta_i(t_{s+1}^i) \le \frac{1}{\xi_i}\Big[(\sigma_i - \bar{k}_i)\|e_i(t_s^i)\|^2 + (\bar{k}_i - \sigma_i)\|e_i(t_s^i) - e_i(t)\|^2\Big]. \tag{4.18}$$

At $t = t_{s+1}^i$, the following inequality holds:

$$\|e_i(t) - e_i(t_s^i)\|^2 \le \frac{W_2 + \bar{k}_i\|e_i(t_s^i)\|^2}{W_1}(e^{W_1(t-t_s^i)} - 1). \tag{4.19}$$

From the above inequality, one obtains

$$\xi_i\eta_i(t_{s+1}^i) - (\sigma_i - \bar{k}_i)\|e_i(t_s^i)\|^2 \le \frac{W_2 + \bar{k}_i\|e_i(t_s^i)\|^2}{W_1}(\bar{k}_i - \sigma_i)(e^{W_1(t_{s+1}^i - t_s^i)} - 1). \tag{4.20}$$

Furthermore, one can derive

$$t_{s+1}^i - t_s^i \geq \frac{1}{W_1} \ln\left[\frac{W_1(\xi_i\eta_i(t_{s+1}^i) - (\sigma_i - \bar{k}_i)\|e_i(t_s^i)\|^2)}{(W_2 + \bar{k}_i\|e_i(t_s^i)\|^2)(\bar{k}_i - \sigma_i)} + 1\right] > 0. \tag{4.21}$$

Under the dynamic event-triggered mechanism, the controlled error system exhibits no Zeno behavior.

5. Numerical simulations

Based on the theoretical analysis presented above, numerical simulations are carried out to verify the correctness and effectiveness of the proposed control strategy.

Consider a heterogeneous neural network, where both the drive layer and the response layer consist of five nodes, and the state of each node is two-dimensional. The system matrices corresponding to $i = 1, \ldots, 5$ are used for this 5-node case, while additional matrices for $i = 6, \ldots, 10$ are provided for the extended network. The initial states are randomly generated within the interval $[-10, 10]$.

The activation functions are chosen as $f^M(\cdot) = (\sin(\cdot), \sin(\cdot))^T$, $g^M(\cdot) = (\cos(\cdot), \cos(\cdot))^T$, $f^S(\cdot) = (\tanh(\cdot), \tanh(\cdot))^T$, $g^S(\cdot) = (\sin(\cdot), \sin(\cdot))^T$. According to the given conditions, the parameters and coefficient matrices are selected as follows: $\xi_1 = 1$, $\xi_2 = 1$, $\xi_3 = 1$, $\xi_4 = 2$, $\xi_5 = 2$; $\sigma_1 = -2$, $\sigma_2 = -2$, $\sigma_3 = -3$, $\sigma_4 = -3$, $\sigma_5 = -3$; $k = 2, \bar{k}_i = 2, \rho_k^{(i)} = 0.7, \eta_i(0) = 0.3, \tau = 0.01$.

The system matrices are given as

$$A_1^M = \begin{pmatrix} 0.2 & -0.1 \\ -0.1 & 0.2 \end{pmatrix}, \quad A_1^S = \begin{pmatrix} 0.2 & 0.1 \\ 0.1 & 0.2 \end{pmatrix}, \quad B_1^M = \begin{pmatrix} -0.1 & -0.2 \\ -0.2 & -0.1 \end{pmatrix},$$

$$B_1^S = \begin{pmatrix} 0.1 & 0.2 \\ 0.2 & 0.1 \end{pmatrix}, \quad C_1^M = \begin{pmatrix} 0.6 & 0 \\ 0 & 0.6 \end{pmatrix}, \quad C_1^S = \begin{pmatrix} 0.5 & 0 \\ 0 & 0.5 \end{pmatrix}.$$

$$A_2^M = \begin{pmatrix} 0.2 & 0.1 \\ 0.1 & 0.2 \end{pmatrix}, \quad A_2^S = \begin{pmatrix} 0.2 & 0.1 \\ 0.1 & 0.2 \end{pmatrix}, \quad B_2^M = \begin{pmatrix} -0.1 & 0.2 \\ 0.2 & -0.1 \end{pmatrix},$$

$$B_2^S = \begin{pmatrix} -0.1 & 0.2 \\ 0.2 & -0.1 \end{pmatrix}, \quad C_2^M = \begin{pmatrix} 0.5 & 0 \\ 0 & 0.5 \end{pmatrix}, \quad C_2^S = \begin{pmatrix} 0.6 & 0 \\ 0 & 0.6 \end{pmatrix}.$$

$$A_3^M = \begin{pmatrix} -0.2 & 0.1 \\ 0.1 & -0.2 \end{pmatrix}, \quad A_3^S = \begin{pmatrix} 0.3 & -0.1 \\ -0.1 & 0.3 \end{pmatrix}, \quad B_3^M = \begin{pmatrix} 0.1 & -0.2 \\ -0.2 & 0.1 \end{pmatrix},$$

$$B_3^S = \begin{pmatrix} -0.1 & 0.3 \\ -0.3 & -0.1 \end{pmatrix}, \quad C_3^M = \begin{pmatrix} 0.7 & 0 \\ 0 & 0.7 \end{pmatrix}, \quad C_3^S = \begin{pmatrix} 0.4 & 0 \\ 0 & 0.4 \end{pmatrix}.$$

$$A_4^M = \begin{pmatrix} -0.2 & -0.1 \\ -0.1 & -0.2 \end{pmatrix}, \quad A_4^S = \begin{pmatrix} -0.2 & -0.1 \\ -0.1 & -0.2 \end{pmatrix}, \quad B_4^M = \begin{pmatrix} 0.1 & 0.2 \\ 0.2 & 0.1 \end{pmatrix},$$

$$B_4^S = \begin{pmatrix} -0.1 & -0.2 \\ -0.2 & -0.1 \end{pmatrix}, \quad C_4^M = \begin{pmatrix} 0.6 & 0 \\ 0 & 0.6 \end{pmatrix}, \quad C_4^S = \begin{pmatrix} 0.7 & 0 \\ 0 & 0.7 \end{pmatrix}.$$

$$A_5^M = \begin{pmatrix} 0.1 & -0.1 \\ -0.1 & 0.1 \end{pmatrix}, \quad A_5^S = \begin{pmatrix} 0.1 & 0.1 \\ 0.1 & 0.1 \end{pmatrix}, \quad B_5^M = \begin{pmatrix} 0.2 & -0.2 \\ -0.2 & 0.2 \end{pmatrix},$$

$$B_5^S = \begin{pmatrix} 0.2 & 0.2 \\ 0.2 & 0.2 \end{pmatrix}, \quad C_5^M = \begin{pmatrix} 0.5 & 0 \\ 0 & 0.5 \end{pmatrix}, \quad C_5^S = \begin{pmatrix} 0.4 & 0 \\ 0 & 0.4 \end{pmatrix}.$$

$$A_6^M = \begin{pmatrix} 0.3 & -0.1 \\ -0.1 & 0.3 \end{pmatrix}, \quad A_6^S = \begin{pmatrix} 0.6 & 0.1 \\ 0.1 & 0.6 \end{pmatrix}, \quad B_6^M = \begin{pmatrix} -0.1 & -0.2 \\ -0.2 & -0.1 \end{pmatrix},$$

$$B_6^S = \begin{pmatrix} 0.1 & 0.2 \\ 0.2 & 0.1 \end{pmatrix}, \quad C_6^M = \begin{pmatrix} -0.6 & -0.3 \\ -0.3 & -0.6 \end{pmatrix}, \quad C_6^S = \begin{pmatrix} 0.5 & 0.3 \\ 0.3 & 0.5 \end{pmatrix}.$$

$$A_7^M = \begin{pmatrix} 0.3 & -0.1 \\ -0.1 & 0.3 \end{pmatrix}, \quad A_7^S = \begin{pmatrix} 0.2 & 0.1 \\ 0.1 & 0.2 \end{pmatrix}, \quad B_7^M = \begin{pmatrix} -0.1 & 0.2 \\ 0.2 & -0.1 \end{pmatrix},$$

$$B_7^S = \begin{pmatrix} 0.4 & 0.2 \\ 0.2 & 0.4 \end{pmatrix}, \quad C_7^M = \begin{pmatrix} 0.7 & 0.3 \\ 0.3 & 0.7 \end{pmatrix}, \quad C_7^S = \begin{pmatrix} -0.6 & -0.4 \\ -0.4 & -0.6 \end{pmatrix}.$$

$$A_8^M = \begin{pmatrix} -0.2 & 0.1 \\ 0.1 & -0.2 \end{pmatrix}, \quad A_8^S = \begin{pmatrix} 0.2 & -0.1 \\ -0.1 & 0.2 \end{pmatrix}, \quad B_8^M = \begin{pmatrix} 0.1 & -0.2 \\ -0.2 & 0.1 \end{pmatrix},$$

$$B_8^S = \begin{pmatrix} -0.1 & -0.2 \\ -0.2 & -0.1 \end{pmatrix}, \quad C_8^M = \begin{pmatrix} -0.7 & 0 \\ 0 & -0.7 \end{pmatrix}, \quad C_8^S = \begin{pmatrix} 0.2 & 0.1 \\ 0.1 & 0.2 \end{pmatrix}.$$

$$A_9^M = \begin{pmatrix} 0.2 & -0.1 \\ -0.1 & 0.2 \end{pmatrix}, \quad A_9^S = \begin{pmatrix} -0.2 & -0.1 \\ -0.1 & -0.2 \end{pmatrix}, \quad B_9^M = \begin{pmatrix} 0.1 & 0.2 \\ 0.2 & 0.1 \end{pmatrix},$$

$$B_9^S = \begin{pmatrix} 0.1 & -0.2 \\ -0.2 & 0.1 \end{pmatrix}, \quad C_9^M = \begin{pmatrix} 1.6 & 0 \\ 0 & 1.6 \end{pmatrix}, \quad C_9^S = \begin{pmatrix} 0.8 & -0.1 \\ -0.1 & 0.8 \end{pmatrix}.$$

$$A_{10}^M = \begin{pmatrix} 0.1 & -0.1 \\ -0.1 & 0.1 \end{pmatrix}, \quad A_{10}^S = \begin{pmatrix} 0.4 & 0.1 \\ 0.1 & 0.4 \end{pmatrix}, \quad B_{10}^M = \begin{pmatrix} -0.2 & -0.2 \\ -0.2 & -0.2 \end{pmatrix},$$

$$B_{10}^S = \begin{pmatrix} 0.3 & -0.3 \\ -0.3 & 0.3 \end{pmatrix}, \quad C_{10}^M = \begin{pmatrix} 0.5 & -0.2 \\ -0.2 & 0.5 \end{pmatrix}, \quad C_{10}^S = \begin{pmatrix} 0.4 & -0.2 \\ -0.2 & 0.4 \end{pmatrix}.$$

Therefore, according to Theorems 1 and 3, the heterogeneous neural network can achieve quasi-synchronization under both static and dynamic event-triggered conditions.

5.1. *Synchronization simulations under static event-triggering*

The following figures present the simulation results under the static event-triggered control scheme based on the prescribed parameters.

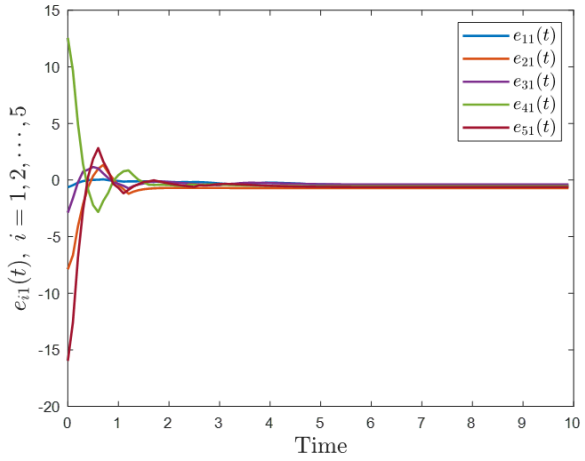

Figure 2. Time responses of the synchronization errors for the first state component under the static event-triggered scheme.

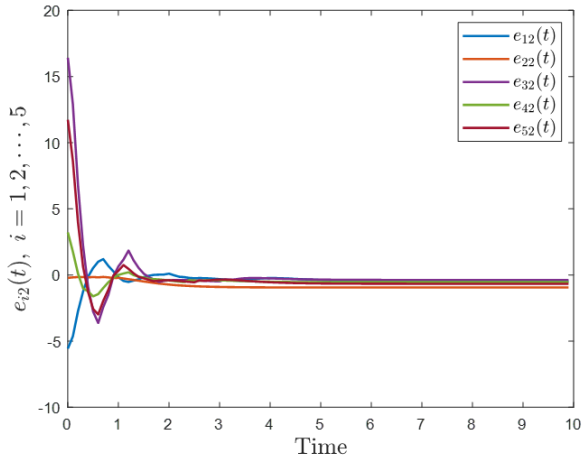

Figure 3. Time responses of the synchronization errors for the second state component under the static event-triggered scheme.

From Figures 2 and 3, it can be observed that under the static event-triggered control strategy, the synchronization errors of both state components converge to a small neighborhood of zero. This indicates that the drive layer and the response layer of the heterogeneous neural network achieve synchronization for all five nodes.

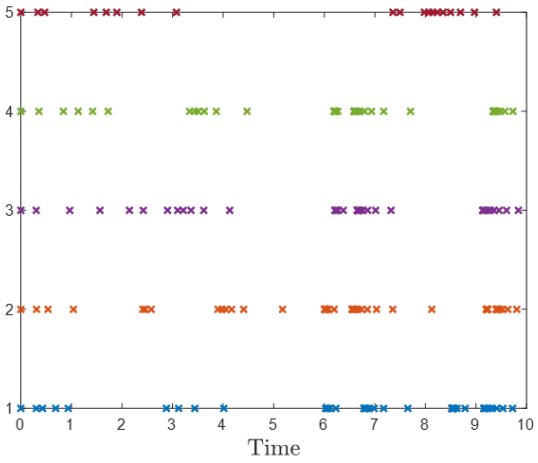

Figure 4. Event-triggering instants of the five nodes under the static event-triggered scheme.

The event-triggered instants under the static event-triggering scheme are illustrated in Figure 4, where the numbers of triggering events for the five nodes are 42, 52, 37, 45, and 19, respectively.

5.2. Synchronization simulations under dynamic event-triggering

The following figures present the simulation results under the dynamic event-triggered control scheme based on the prescribed parameters.

From Figures 5 and 6, it can be observed that under the dynamic event-triggered control strategy, the synchronization errors of both state components converge to zero. This indicates that the drive layer and the response layer of the heterogeneous neural network can achieve node-to-node synchronization for all five nodes.

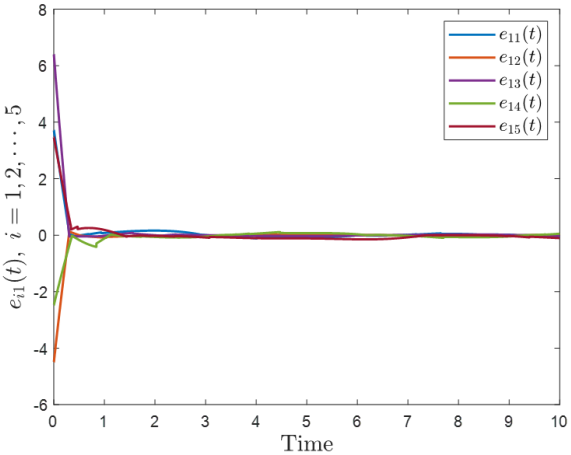

Figure 5. Time responses of the synchronization errors for the first state component under the dynamic event-triggered scheme.

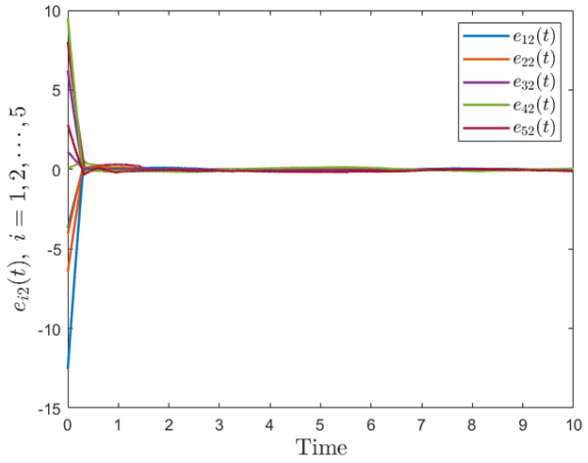

Figure 6. Time responses of the synchronization errors for the second state component under the dynamic event-triggered scheme.

Compared with the static event-triggered strategy, the dynamic event-triggered scheme achieves a faster synchronization speed, demonstrating its superiority in improving convergence performance.

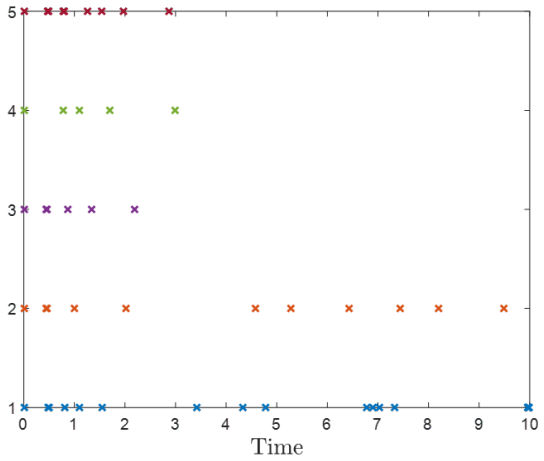

Figure 7. Event-triggering instants of the five nodes under the dynamic event-triggered scheme.

As shown in Figure 7, the numbers of triggering events for the five nodes under the dynamic event-triggered scheme are 16, 11, 6, 5, and 9, respectively. Compared with the static event-triggered strategy, the dynamic event-triggered mechanism significantly reduces the triggering frequency, thereby lowering communication and computation costs.

To further demonstrate the scalability and effectiveness of the proposed hybrid event-triggered impulsive control strategy, a heterogeneous neural network with 10 nodes is additionally considered. The synchronization error trajectories of the 10-node network are presented in Figures 8 and 9. It can be observed that the synchronization errors converge to zero, indicating that the proposed control

method remains effective for networks with larger sizes.

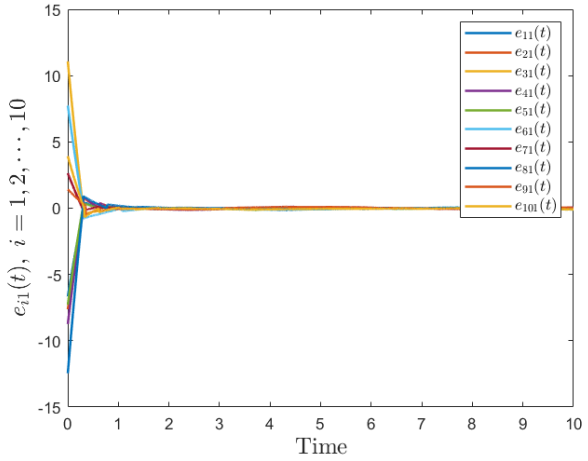

Figure 8. Time responses of the synchronization errors for the first state component in the 10-node heterogeneous neural network.

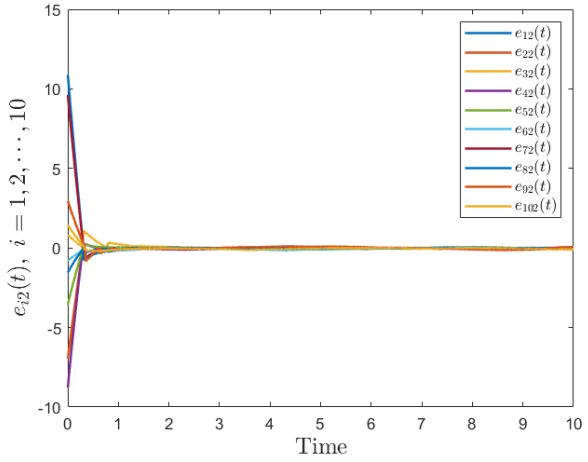

Figure 9. Time responses of the synchronization errors for the second state component in the 10-node heterogeneous neural network.

From Figure 10, it can be observed that the adaptive control gain varies dynamically and converges to a bounded value. This indicates that the proposed adaptive event-triggered impulsive control strategy possesses good self-adjustment capability, enabling it to adapt to different operating conditions effectively.

Based on the above numerical simulations, it is concluded that both static and dynamic event-triggered control schemes can realize node-to-node synchronization between the drive layer and the response layer of the heterogeneous neural network. Moreover, by introducing the dynamic variable $\eta_i(t)$ to adjust the triggering threshold adaptively, the dynamic event-triggered strategy achieves a faster

synchronization speed with fewer triggering events compared with the static scheme.

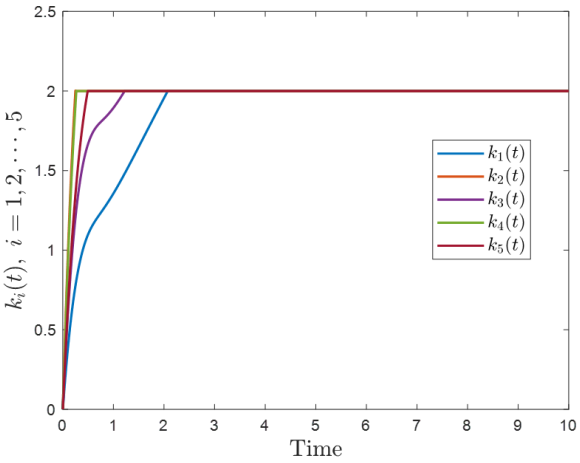

Figure 10. Evolution of the adaptive control gain under the dynamic event-triggered mechanism.

6. Conclusions

This paper investigates the synchronization control problem of heterogeneous neural networks and proposes a novel hybrid control strategy that integrates adaptive state feedback with impulsive control. Through rigorous theoretical analysis, the effectiveness of the proposed controller is verified under both static and dynamic event-triggered mechanisms, and quasi-synchronization of the networked system is achieved. Moreover, the proposed dynamic event-triggered strategy effectively excludes Zeno behavior. Numerical simulation results further validate the correctness of the theoretical analysis, demonstrating that the proposed method exhibits significant advantages in reducing communication burden and energy consumption. These results indicate that the developed control framework provides an efficient and practical solution for synchronization control of heterogeneous neural networks. Future research will focus on the development of more efficient control strategies to address robust synchronization control of heterogeneous neural networks in more complex environments. In addition, reformulating the stability conditions within a linear matrix inequality (LMI) framework is also a promising direction for future research.

Use of AI tools declaration

The authors declare they have not used Artificial Intelligence (AI) tools in the creation of this article.

Acknowledgments

This work was supported by the National Natural Science Foundation of China (Grant Nos. 12272092 and 12572067).

Conflict of interest

Professor Fang Han is a Guest Editor of special issue "Neural dynamical modeling and brain-inspired intelligence" for Electronic Research Archive. She was not involved in the editorial review and the decision to publish this article. The authors declare there are no conflicts of interest.

References

1. Z. D. Wang, Y. R. Liu, M. Z. Li, X. H. Liu, Stability analysis for stochastic Cohen–Grossberg neural networks with mixed time delays, *IEEE Trans. Neural Networks*, **17** (2006), 814–820. https://doi.org/10.1109/TNN.2006.872355
2. J. H. Li, H. L. Dong, Z. D. Wang, X. Y. Bu, Partial-neurons-based passivity-guaranteed state estimation for neural networks with randomly occurring time delays, *IEEE Trans. Neural Networks Learn. Syst.*, **31** (2020), 3747–3753. https://doi.org/10.1109/tnnls.2019.2944552
3. A. I. Luppi, F. E. Rosas, P. A. M. Mediano, D. K. Menon, E. A. Stamatakis, Information decomposition and the informational architecture of the brain, *Trends Cognit. Sci.*, **28** (2024), 352–368. https://doi.org/10.1016/j.tics.2023.11.005
4. T. Chen, L. Zhu, C. Deng, R. Cao, Y. Wang, S. Zhang, Sam-adapter: adapting segment anything in underperformed scenes, in *2023 IEEE/CVF International Conference on Computer Vision Workshops (ICCVW)*, (2023), 3359–3367. https://doi.org/10.1109/ICCVW60793.2023.00361
5. X. Fu, S. Zhang, T. Chen, Y. Lu, L. Zhu, X. Zhou, Panoptic NeRF: 3D-to-2D label transfer for panoptic urban scene segmentation, in *2022 International Conference on 3D Vision (3DV)*, (2022), 1–11. https://doi.org/10.1109/3DV57658.2022.00042
6. T. Wu, S. He, J. Liu, S. Sun, K. Liu, Q. Han, A brief overview of ChatGPT: the history, status quo and potential future development, *IEEE/CAA J. Autom. Sin.*, **10** (2023), 1122–1136. https://doi.org/10.1109/jas.2023.123618
7. L. Ding, Q. Han, X. Ge, X. Zhang, An overview of recent advances in event-triggered consensus of multiagent systems, *IEEE Trans. Cybern.*, **48** (2017), 1110–1123. https://doi.org/10.1109/tcyb.2017.2771560
8. X. M. Zhang, Q. L. Han, X. Ge, D. Ding, L. Ding, D. Yue, Networked control systems: a survey of trends and techniques, *IEEE/CAA J. Autom. Sin.*, **7** (2019), 1–17. https://doi.org/10.1109/jas.2019.1911651
9. X. Ge, Q. Han, L. Ding, Y. Wang, X. Zhang, Dynamic event-triggered distributed coordination control and its applications: a survey of trends and techniques, *IEEE Trans. Syst. Man Cybern.: Syst.*, **50** (2020), 3112–3125. https://doi.org/10.1109/tsmc.2020.3010825
10. D. H. Chang, Y. Geng, Distributed data-driven iterative learning control for multi-agent systems with unknown input-output coupled parameters, *Electron. Res. Arch.*, **33** (2025), 867–889. https://doi.org/10.3934/era.2025039
11. Y. Gong, Consensus control of multi-agent systems with delays, *Electron. Res. Arch.*, **32** (2024), 4887–4904. https://doi.org/10.3934/era.2024224

12. T. M. Priyanka, A. Gowrisankar, Multifractality on chaos and bursting oscillations in 4D heterogeneous Hopfield neural network with a memristor-based adaptive activation function, *Neurocomputing*, **658** (2025), 131780. https://doi.org/10.1016/j.neucom.2025.131780

13. S. Sun, Z. Wang, C. Jin, Y. Feng, M. Xiao, C. Zheng, Event-triggered synchronization of a two-layer heterogeneous neural network via hybrid control, *Commun. Nonlinear Sci. Numer. Simul.*, **123** (2023), 107279. https://doi.org/10.1016/j.cnsns.2023.107279

14. M. Shen, C. Wang, Q. G. Wang, H. Yan, G. Zong, Z. H. Zhu, Fault-tolerant synchronization control of switched complex networks by a proportional–integral intermediate observer approach, *IEEE Trans. Cybern.*, **55** (2025), 4689–4698. https://doi.org/10.1109/TCYB.2025.3591393

15. N. Li, J. Cao, New synchronization criteria for memristor-based networks: adaptive control and feedback control schemes, *Neural Networks*, **61** (2015), 1–9. https://doi.org/10.1016/j.neunet.2014.08.015

16. Z. Yang, B. Luo, D. Liu, Y. Li, Adaptive synchronization of delayed memristive neural networks with unknown parameters, *IEEE Trans. Syst. Man Cybern.: Syst.*, **50** (2017), 539–549. https://doi.org/10.1109/tsmc.2017.2778092

17. S. Wen, T. Huang, X. Yu, M. Z. Q. Chen, Z. Zeng, Aperiodic sampled-data sliding-mode control of fuzzy systems with communication delays via the event-triggered method, *IEEE Trans. Fuzzy Syst.*, **24** (2015), 1048–1057. https://doi.org/10.1109/tfuzz.2015.2501412

18. S. Wen, T. Huang, X. Yu, M. Z. Q. Chen, Z. Zeng, Sliding-mode control of memristive Chua's systems via the event-based method, *IEEE Trans. Circuits Syst. II Express Briefs*, **64** (2016), 81–85. https://doi.org/10.1109/tcsii.2016.2538727

19. P. Wang, Q. Zhang, H. Su, Aperiodically intermittent control for synchronization of discrete-time delayed neural networks, *J. Franklin Inst.*, **359** (2022), 4915–4937. https://doi.org/10.1016/j.jfranklin.2022.04.033

20. Y. Jiang, S. Luo, Periodically intermittent synchronization of stochastic delayed neural networks, *Circuits Syst. Signal Process.*, **36** (2017), 1426–1444. https://doi.org/10.1007/s00034-016-0377-5

21. Y. W. Wang, Y. Lei, T. Bian, Z. Guan, Distributed control of nonlinear multiagent systems with unknown and nonidentical control directions via event-triggered communication, *IEEE Trans. Cybern.*, **50** (2019), 1820–1832. https://doi.org/10.1109/TCYB.2019.2908874

22. L. Liu, H. Bao, Event-triggered impulsive synchronization of coupled delayed memristive neural networks under dynamic and static conditions, *Neurocomputing*, **504** (2022), 109–122. https://doi.org/10.1016/j.neucom.2022.06.098

23. Y. Zhou, Z. Zeng, Event-triggered impulsive control on quasi-synchronization of memristive neural networks with time-varying delays, *Neural Networks*, **110** (2019), 55–65. https://doi.org/10.1016/j.neunet.2018.09.014

24. Y. Zhou, H. Zhang, Z. Zeng, Quasisynchronization of memristive neural networks with communication delays via event-triggered impulsive control, *IEEE Trans. Cybern.*, **52** (2020), 7682–7693. https://doi.org/10.1109/tcyb.2020.3035358

25. A. Kazemy, J. Lam, X. M. Zhang, Event-triggered output feedback synchronization of master–slave neural networks under deception attacks, *IEEE Trans. Neural Networks Learn. Syst.*, **33** (2020), 952–961. https://doi.org/10.1109/TNNLS.2020.3030638

26. Y. Zhou, H. Zhang, Z. Zeng, Synchronization of memristive neural networks with unknown parameters via event-triggered adaptive control, *Neural Networks*, **139** (2021), 255–264. https://doi.org/10.1016/j.neunet.2021.02.029

27. W. He, B. Xu, Q. L. Han, F. Qian, Adaptive consensus control of linear multiagent systems with dynamic event-triggered strategies, *IEEE Trans. Cybern.*, **50** (2019), 2996–3008. https://doi.org/10.1109/tcyb.2019.2920093

28. H. Zhang, T. Ma, G. B. Huang, Z. Wang, Robust global exponential synchronization of uncertain chaotic delayed neural networks via dual-stage impulsive control, *IEEE Trans. Syst. Man Cybern. Part B Cybern.*, **40** (2009), 831–844. https://doi.org/10.1109/tsmcb.2009.2030506

29. Z. Tang, J. H. Park, J. Feng, Impulsive effects on quasi-synchronization of neural networks with parameter mismatches and time-varying delay, *IEEE Trans. Neural Networks Learn. Syst.*, **29** (2017), 908–919. https://doi.org/10.1109/tnnls.2017.2651024

30. W. Zhu, D. Wang, L. Liu, G. Feng, Event-based impulsive control of continuous-time dynamic systems and its application to synchronization of memristive neural networks, *IEEE Trans. Neural Networks Learn. Syst.*, **29** (2017), 3599–3609. https://doi.org/10.1109/tnnls.2017.2731865

AIMS Press